

## Effects of build parameters on compression properties for ULTEM 9085 parts by fused deposition modeling

Krishna P. Motaparti <sup>1</sup>, Gregory Taylor <sup>1</sup>, Ming C. Leu <sup>1</sup>, K. Chandrashekhara <sup>1</sup>, James Castle <sup>2</sup>  
and Mike Matlack <sup>2</sup>

<sup>1</sup>Department of Mechanical and Aerospace Engineering, Missouri University of Science and  
Technology, Rolla, Missouri, USA

<sup>2</sup>The Boeing Company, St Louis, Missouri, USA

### Abstract

It has been observed by various researchers that parts fabricated by the Fused Deposition Modeling (FDM) process have anisotropic properties. The research presented in the present paper was aimed to study the compression properties of FDM parts and to comprehend their dependence on build parameters. In this study Ultem 9085 was used as the material to fabricate both solid and sparse-build coupons with variations in build direction, raster angle and air gap. A full factorial experimental design was used to study the individual and combined effects of these build parameters on the mechanical properties of the coupons. The mechanical properties studied include compressive yield strength, compressive modulus, compressive strength/mass ratio, and compressive modulus/mass ratio. Besides the obtained test data, qualitative observation and reasoning was used to help understand how the compression properties are affected by the build parameters.

### 1. Introduction

Additive manufacturing (or 3D printing) is a method of fabricating three-dimensional prototypes or parts through the deposition of layers upon layers of material. Currently, additive manufacturing has spread into numerous industries and is quickly becoming a widely accepted manufacturing technique for more than just prototypes. Contrary to subtractive manufacturing techniques, additive manufacturing has a greatly reduced material requirement due to the layer-by-layer building process. Additive manufacturing has a variety of building techniques, but one in particular, Fused Deposition Modeling (FDM), is often utilized for the fabrication of thermoplastic components. The fabrication is controlled by machine code generated from a CAD model in STL (STereo Lithography) format. With the build parameters and STL file, an FDM machine fabricates the physical part through an extrusion of the thermoplastic material from a nozzle head. In the FDM machine of this study, the build platform has motion in the vertical Z direction whereas the nozzle head has motion constrained to the horizontal plane (i.e. in X and Y directions).

Currently, there is a need to understand the mechanical behavior of FDM specimens and researchers have been studying the dependence on build parameters such as build direction, raster orientation, raster width, layer thickness, oven temperature, etc. [1-10]. Schopper *et al.* [1] studied the effect of build direction on the compression properties of FDM specimens and they reported that the yield strength and compressive modulus of specimens built in the horizontal direction were higher in comparison to the specimens built in the vertical direction. Also, according to Bagsik *et al.* [2], the tensile properties of specimens made of Ultem 9085 were

higher in all build directions using a negative air gap. Lee *et al.* [3] conducted a case study by using Taguchi method to investigate the build parameters in order to achieve optimum performance for a compliant ABS prototype. Lee *et al.* [4] compared the compressive strengths of parts made by FDM, inkjet printing, and nano composite deposition system (NCDS). They reported that the parts made by FDM had high compressive strength in comparison to the other processes. Ognzan *et al.* [5] studied the effects of layer thickness, deposition angle, and infill percentage on the maximum flexural force in FDM specimens made of polylactic acid (PLA). They concluded that layer thickness has the maximum effect on the flexural strength followed by the interaction between deposition angle and infill percentage. A relationship between the total costs of FDM parts and their mechanical properties was established by Rauta *et al.* [6] to enable the engineers to decide on proper build orientations so that FDM parts can be fabricated with good mechanical properties at low manufacturing costs. The effects of raster angle, oven temperature, and raster width on the properties of FDM parts made of ABS were studied using a bacterial foraging technique by Panda *et al.* [7] in order to determine optimal build parameter settings to achieve good strength. Rayegani *et al.* [8] used the group method for prediction purposes and developed a functional relationship between build parameters and the part's tensile strength for the FDM process. During the production of components using FDM, factors like build time and surface roughness play an important role. Several studies were conducted to optimize these factors using different build parameters. Anitha *et al.* [9] used Taguchi method to study the various build parameters used in FDM that affect the quality of the fabricated part. The quality was measured in terms of the surface roughness of the part and it was found that layer thickness, raster width, and speed of deposition influence the part quality with layer thickness having the maximum effect. Similar experiments conducted by Vasudevarao *et al.* [10] revealed that part orientation also affects surface finish but air gap does not have significant influence on surface quality. The technical literature mostly contains studies that analyze the measured data from experiments, and there have been very few qualitative reasoning studies for the observed part properties.

The main objective of this research is to study how various build parameters including build direction, raster angle, and air gap affect the compressive modulus and yield strength of FDM produced Ultem 9085 specimens with solid and sparse build. The study includes a full-factorial design of experiments to help understand how much of an effect, if any, the build parameters have on the compression properties.

## **2. Material and Methods**

### **2.1. Additive manufacturing machine and material**

In this study, all specimens were fabricated with a Fortus 400mc (Stratasys). The machine is capable of building components within a 406 mm x 356 mm x 4.6 mm (16" x 14" x 16") build envelope and with a  $\pm 0.0015$  mm/mm accuracy. While the Fortus 400mc is able to build with many thermoplastic materials such as ABS, Ultem, Polycarbonate (PC), and PPSF, this study used Ultem 9085 as the specimen material. Ultem 9085 is regarded as a high-performance thermoplastic with high temperature capacity and good strength-to-weight ratio. With the fabrication of Ultem 9085 specimens, a breakaway support material was used. Fabrication of the specimens consisted of the following steps:

1. **Pre-processing:** Three-dimensional models of the test specimens are modeled in CAD software (SolidWorks) and exported as a Stereo Lithography (STL) file. The STL file is taken as input into Statasys Insight 9.1 software where the fabrication tool path is generated from user-specified build parameters. Figure 1 shows a potential schematic for a rectangular layer of FDM component.
2. **Fabrication:** After pre-processing, the STL file is sent to the Fortus 400mc using Stratasys Insight and Control Center Job Processing and Management software. The specimen is then fabricated using the FDM process.
3. **Post-processing:** After fabrication, the support structure is mechanically removed from the model and the specimen is finished.

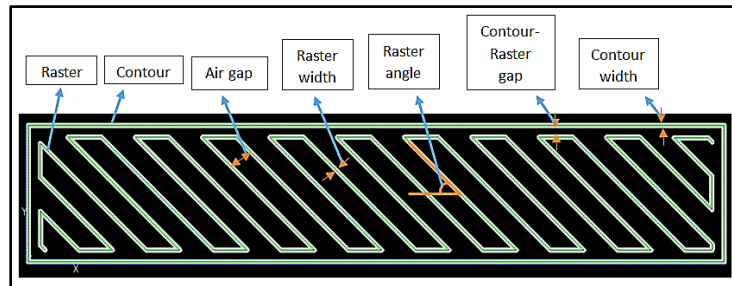


Figure 1. FDM layer schematic in Insight software showing different build parameters

## 2.2. Specimen fabrication

For this study, the Ultem 9085 specimens were built with two build directions, horizontal and vertical. For the horizontal-build, specimens are fabricated with the build direction parallel to the compression load to be applied later. For the vertical-build, specimens are fabricated with the build direction perpendicular to the compression load to be applied. Raster angle varied with either ( $45^\circ$ ,  $-45^\circ$ ) and ( $0^\circ$ ,  $90^\circ$ ). Air gap varied with  $-0.00635$  mm ( $-0.00025''$ ),  $-0.0127$  mm ( $-0.0005''$ ), or  $-0.01905$  mm ( $-0.00075''$ ) for solid specimens but was held at a constant  $2.54$  mm ( $0.1''$ ) for the sparse specimens. Raster width and contour width were both held at a constant  $0.508$  mm ( $0.02''$ ) for all specimens. Specimens were fabricated with a  $38.1$  mm x  $38.1$  mm ( $1.5''$  x  $1.5''$ ) cross-section and  $25.4$  mm ( $1''$ ) height as shown in Figure 2. Compression tests were performed with a  $1.27$  mm/min ( $0.05$  in/min) loading rate and were stopped when the specimen had over 10% strain. Effective modulus was calculated as stress divided by strain in the elastic region and effective yield strength was calculated as strength at 0.2% offset.

For all specimens, compression tests were conducted on an Instron 5980 which records the load and extension for each test specimen. Instron software was then used to calculate and plot the stress vs. strain curve for each specimen. Stress is defined as the compressive load per unit area of the specimen cross-section. Compressive strain is defined as the ratio of compressive deformation to the gage length of the test specimen.

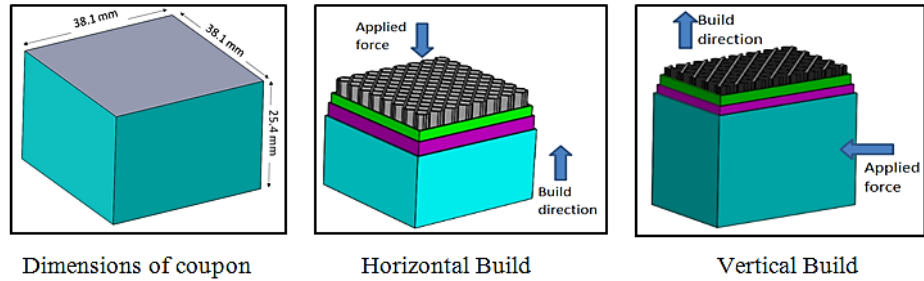


Figure 2. Dimensions, horizontal-build specimen, and vertical-build specimen used in this study

### 2.3. Design of experiments – factors and levels

In design of experiments, independent variables, also known as factors, and variations for these variables, also known as levels, are established. This study splits the specimens into two experiments, solid and sparse specimens.

For the solid specimen case, three factors including build direction, raster angle, and air gap were used (Table 1). Build direction has two levels, horizontal and vertical. Raster angle has two levels, (0°, 90°) and (45°, -45°). Air gap has three levels, -0.00635 mm (-0.00025”), -0.0127 mm (-0.0005”) and -0.01905 mm (-0.00075”). While increasing the magnitude of the negative air gap in the solid specimens will generally increase the strength, the negative air gap will greatly decrease the surface quality of the specimens when the air gap reaches a certain limit (-0.01905 mm for the Fortus 400mc). A full-factorial experiment was performed using the 12 combinations with replications of 5 samples for each combination.

Table 1. Factors and levels for solid build style

Factors	Levels (5 Replications)		
	-1	0	1
Build direction	Horizontal	-	Vertical
Raster angle (degrees/degrees)	0/90	-	45/-45
Air gap (mm)	-0.00635	-0.0127	-0.01905

In the sparse case, two factors including build direction and raster angle were used (Table 2). Unlike the solid case, the air gap was fixed at 2.54 mm (0.1”). Build direction has two levels, horizontal and vertical. Raster angle has two levels, (0°, 90°) and (45°, -45°). A full-factorial experiment was performed using the 4 combinations with replications of 5 samples for each combination.

Table 2. Factors and levels for sparse build style

Factors	Levels (5 Replications)		
	-1	0	1
Build direction	Horizontal	-	Vertical
Raster angle (degrees/degrees)	0/90	-	45/-45

### 3. Experimental Results

Two types of experiments were performed in this study. The first experiment was performed to study the effects of build direction and temperature on both solid and sparse compression properties of FDM specimens. The second experiment was aimed at understanding the effects build parameters including build direction, raster angle, and air gap on the compression properties of FDM specimens. The second experiment was further divided into solid and sparse specimens.

#### 3.1. Effects of build style and temperature

Five specimens were tested for each combination of solid/sparse, build direction, and temperature. Build styles included horizontal-build and vertical-build while temperatures included 24°C (75°F), 82°C (180°F), and 121°C (250°F). The obtained compressive modulus, yield strength, specific modulus, and specific yield strength of the specimens were averaged and plotted along with standard deviation.

From compression test results shown in Figure 3, at all three temperatures [24°C (75°F), 82°C (180°F), 121°C (250°F)], the yield strength, compression modulus, strength/mass ratio, and modulus/mass ratio of the horizontal-build specimens (S-H and SP-H) are higher in comparison to the corresponding vertical-build specimens (S-V and SP-V). The specimens with S-H build style (solid specimen with horizontal-build) exhibits the highest strength and modulus at each respective temperature. These results clearly indicate that both solid/sparse build and build direction affect the compression properties of FDM specimens.

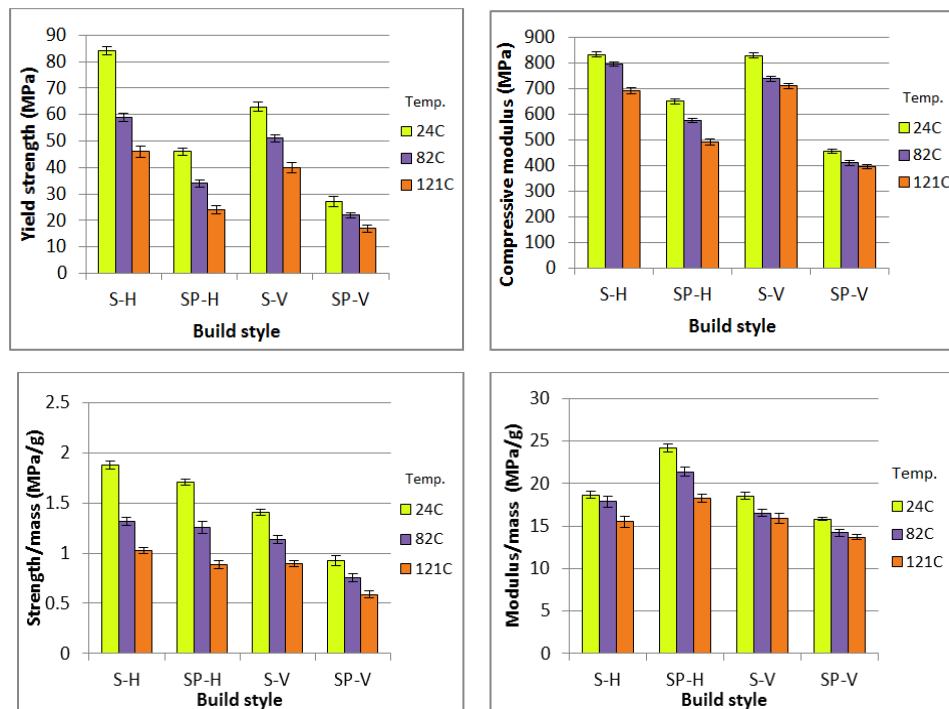


Figure 3. Comparison of compression properties for solid and sparse specimens with different build directions for three temperatures (S indicates a solid specimen, SP indicates a sparse specimen, H indicates horizontal-build direction, and V indicates vertical-build direction)

The results show the yield strength of the solid specimen decreases with increase in temperature. In the case of horizontal-build specimens, the yield strength decreases more than the vertical-build specimens for each respective temperature. This indicates that the vertical-build specimens display a relatively higher resistance to temperature in comparison to the horizontal-build specimens, whereas horizontal-build specimens display relatively higher strength.

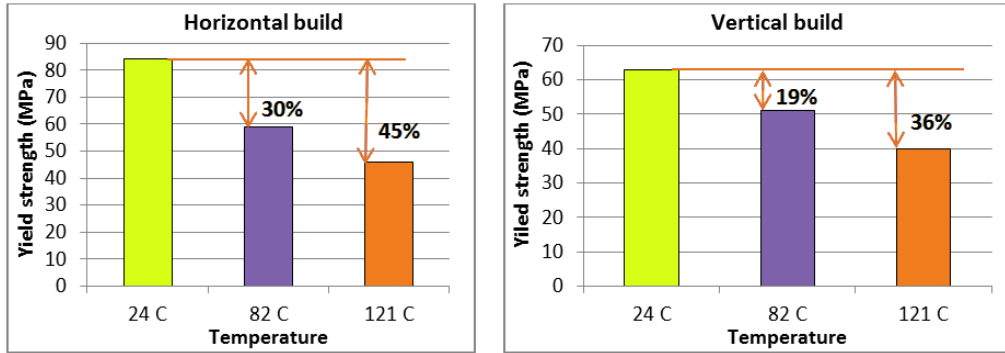


Figure 4. Decrease in yield strength of horizontal-build and vertical-build solid specimens

### 3.2. Effects of build direction, raster angle and air gap

A second type of experiment was designed to conduct compression tests on both solid and sparse specimens with varying build parameters including build direction, raster angle, and air gap (air gap constant for sparse specimens). A full-factorial design of experiment was used for both solid and sparse specimens and the effects of the parameters were studied.

#### 3.2.1. Solid-build style

Compression tests were conducted on the FDM fabricated solid specimens. A total of 60 specimens were tested for 12 different combinations of solid build parameters and 5 replications for each set of parameters. The study investigated compression properties including modulus, yield strength, specific modulus, and specific yield strength. The full-factorial experiment was used for the determination of the main effects and the interactions among the parameters. Main effect is defined as the effect of an independent variable on a response variable averaging across different levels of other independent variables. Independent variables include build direction, raster angle, and air gap for the solid specimen case. If the effect of one independent variable on the response variable is dependent on the value of another independent variable, those two variables are said to exhibit interaction. Yield strength was the only response variable considered during the experiment. All results were analyzed with JMP 11. Results from the statistical software are given in Table 3. The p-value [19] defines the level of significance within a statistical test and represents the probability of a factor affecting the outcome (response variable).

Table 3. Effects table from JMP 11 for solid specimen case

Factors	Sum of Squares	F Ratio	p-value
Build direction	4775.5037	8392.691	<.0001
Raster angle	343.6323	603.9153	<.0001
Air gap	6.9546	3.4946	0.0816
Build*Raster	249.6281	438.708	<.0001
Build*Air gap	1.5674	2.7547	0.1019
Raster*Air gap	0.7047	1.2385	0.2699

For this statistical experiment, if the p-value is less than 0.05 (for a significance level of 95%), the corresponding factor has a significant effect on the response variable. All p-values less than 0.05 are highlighted in red to indicate main effects and/or interaction. The effects table indicates an interaction between build direction and raster angle, which means that the effect of raster angle on the response variable is dependent on the build direction used for the specimen. The interaction of these parameters is described below in detail.

**Interaction of build direction and raster angle:** The two different raster angles evaluated in this experiment included (0°, 90°) and (45°, -45°) for both horizontal-build and vertical-build solid specimens. The results are shown in Figures 6 and 7.

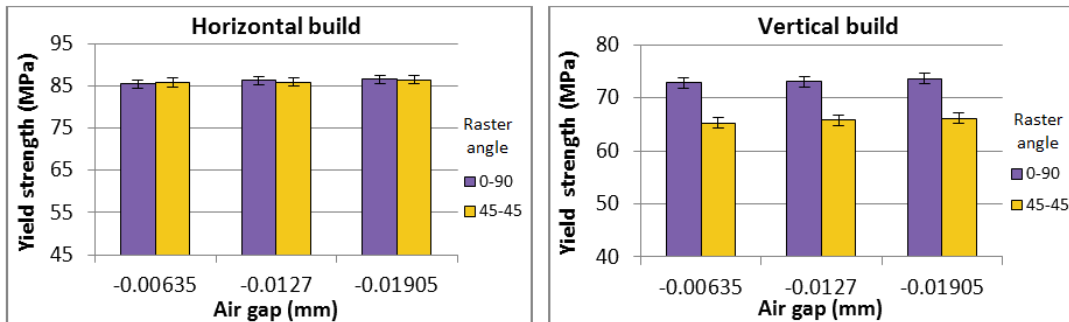


Figure 6. Interaction of build direction and raster angle on yield strength of solid specimens

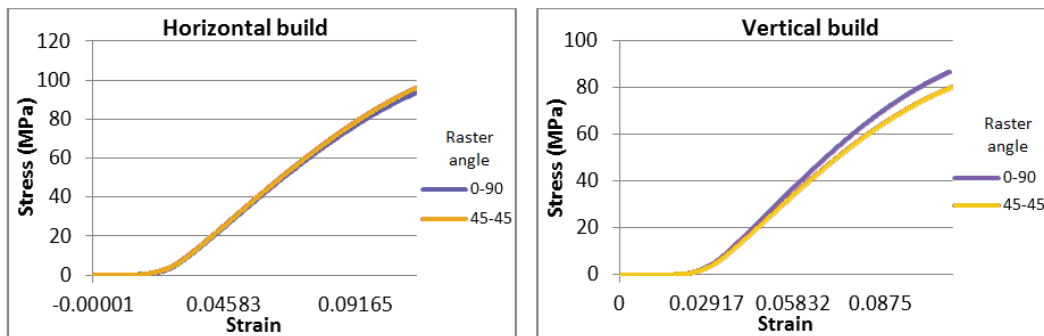


Figure 7. Sample compression stress-strain curves for horizontal-build and vertical-build solid specimens (air gap = -0.00635mm)

*Horizontal build:* According to the graphs in Figures 6 and 7, the horizontal-build specimens with  $(0^\circ, 90^\circ)$  and  $(45^\circ, -45^\circ)$  raster angles have very small differences in the yield strength, and the trend remains the same for different values of air gap. This occurs because in the case of horizontal-build specimens, the applied load is perpendicular to the layer in which the rasters are present, and the internal structure for resisting the external load is essentially the same for different raster angles; refer to Figure 8.

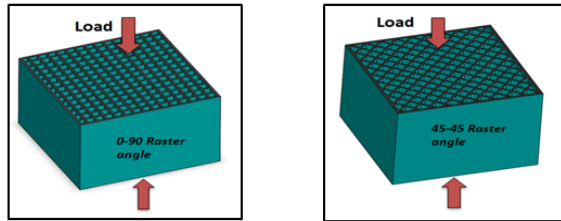


Figure 8. Physical models for horizontal-build compression solid specimens with  $(0^\circ, 90^\circ)$  and  $(45^\circ, -45^\circ)$  raster angles

*Vertical build:* From the graphs in Figures 6 and 7, the vertical-build specimens with  $(0^\circ, 90^\circ)$  raster angles exhibit about 12% higher yield strength in comparison to the specimens with  $(45^\circ, -45^\circ)$  raster angles. The trend remains the same for different air gaps. This indicates that the specimens built with  $(0^\circ, 90^\circ)$  raster angle offer more resistance to deformation in comparison to the specimens built with  $(45^\circ, -45^\circ)$  raster angle. Figure 9 illustrates the  $(0^\circ, 90^\circ)$  vs.  $(45^\circ, -45^\circ)$  raster angle in vertical-build solid specimens.

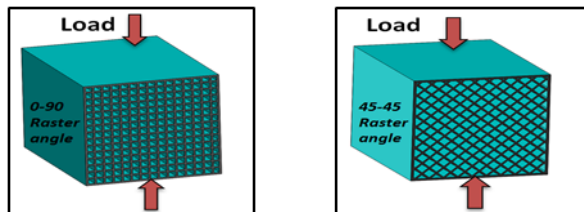


Figure 9. Physical models for vertical-build solid specimens with  $(0^\circ, 90^\circ)$  and  $(45^\circ, -45^\circ)$  raster angles

**Effect of air gap:** The three air gaps evaluated in this experiment included  $-0.00635$  mm ( $-0.00025''$ ),  $-0.0127$  mm ( $-0.0005''$ ) and  $-0.01905$  mm ( $-0.00075''$ ) for both horizontal-build and vertical-build solid specimens. The results are shown in Figures 10 and 11.

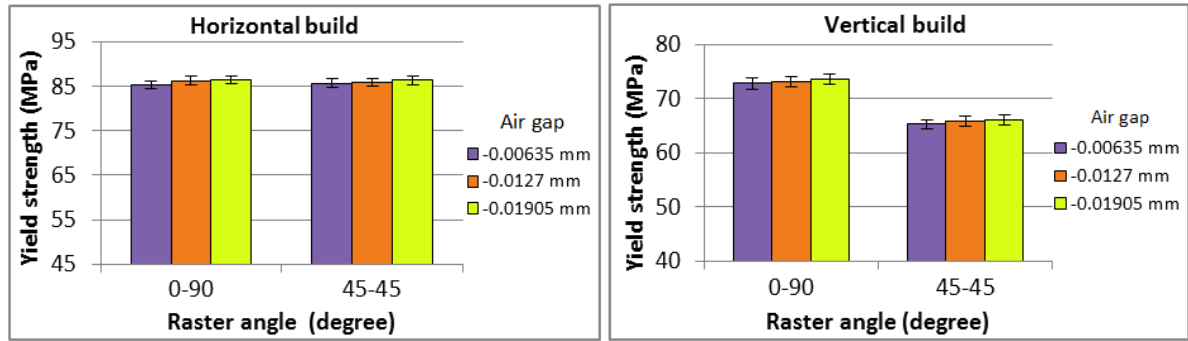


Figure 10. Effect of air gap on yield strength for solid specimens

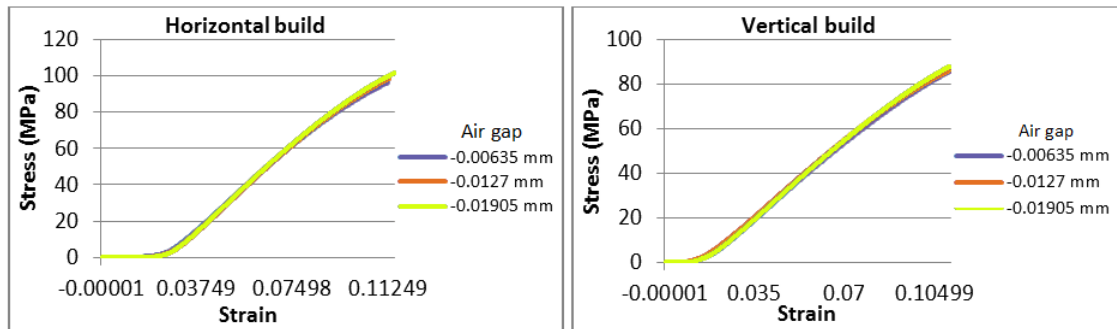


Figure 11. Stress-strain curves at different air gaps for horizontal-build and vertical-build specimens, where the raster angle was (0°, 90°)

*Horizontal build:* From Figures 10 and 11 and the effects table in Table 3, it can be seen that in the case of horizontal-build solid specimens, the effect of air gap is not significant with a p-value > 0.05. The trend remains the same for both (0°, 90°) and (45°, -45°) raster angles. This indicates that the variation in air gap between the rasters does not have a significant effect on the failure due to inter-layer sliding in solid specimens.

*Vertical build:* The effect of air gap in vertical-build is also not significant and the trend remains the same for (0°, 90°) and (45°, -45°) raster angles. As indicated by the effects table, the influence of air gap on the yield strength is not significant (p-value > 0.05), i.e., there is no main effect of air gap for vertical-build. This indicates that the variation in air gap between the rasters also does not have a significant effect on the failure due to buckling in solid specimens.

### 3.2.2. Sparse-build style

Compression tests were conducted on the FDM fabricated sparse specimens. A total of 20 specimens were tested for 4 different combinations of sparse-build parameters and 5 replications for each set of parameters. The air gap was held at a constant 2.54 mm (0.1”) for all sparse samples. A full-factorial experiment was conducted to determine the statistical significance of the build direction and raster angle. The effects table created in JMP 11 shows the main effects and interaction of the two parameters (Table 4).

Table 4. Effects table from JMP 11 for sparse specimen case

Factor	Sum of Squares	F Ratio	p- Value
Build direction	1062.88	814.62	<.0001
Raster angle	138.33	106.02	<.0001
Build*Raster	175.23	134.3	<.0001

From the P-values in Table 4, the build direction and raster angle and their interaction each have a significant effect (p-value < 0.05) on the yield strength. The interaction of these parameters is described below in detail.

**Interaction of build direction and raster angle:** From Figures 12 and 13, the strength of specimens built in horizontal direction is 19% to 40% higher than that in vertical direction for sparse specimens. This behavior is similar to the one observed in the case of solid specimens, and it is expected since the layers in vertical-build specimens fail due to buckling of layers, whereas in the case of horizontal-build specimens, the failure occurs due to inter-layer sliding. Similar to solid-build style, a change in raster angle on horizontal-build sparse specimens shows only a small difference in the yield strength of the sparse specimen. This is expected as the applied compression force acts perpendicular to the layer in which the rasters are present. Similar to solid specimens, the internal structure for resisting the external load is essentially the same for different raster angles. However, in the case of vertical-build, the effect of raster angle is more pronounced as seen in Figure 12. The specimens with (0°, 90°) raster angle have about 30% higher yield strength in comparison to the specimens with (45°, -45°) raster angle. This indicates that the (0°, 90°) rasters produce relatively stiffer specimens compared to (45°, -45°) raster specimens.

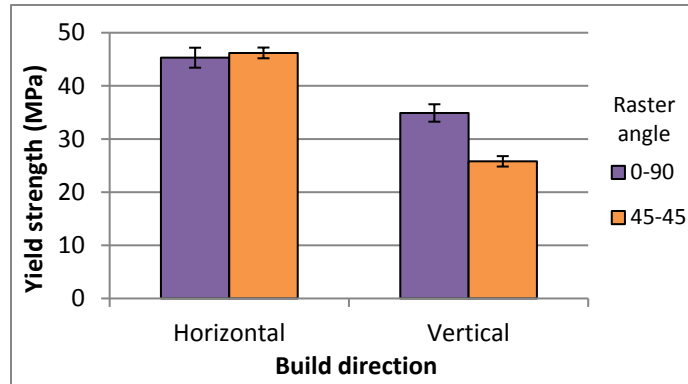


Figure 12. Effect of raster angle for horizontal-build and vertical-build sparse specimens

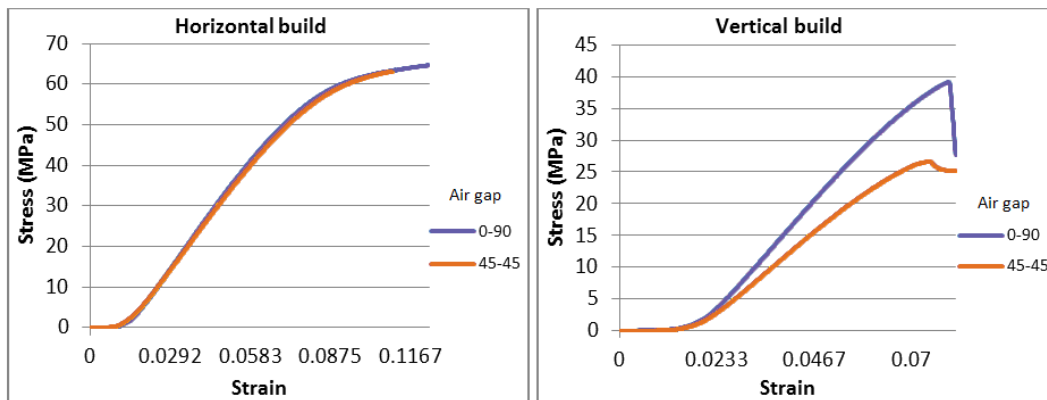


Figure 13. Sample stress-strain curves for horizontal-build and vertical-build sparse specimens

### 3.2.3. Failure of vertical-build sparse specimens

From the above results, the mechanical properties of vertical-build sparse specimens with (0°, 90°) raster angle are higher in comparison to the specimens with (45°, -45°) raster angle in compression tests. In the case of (0°, 90°) raster angle, only the rasters deposited perpendicular to the loading surface will resist the load, but in the case of (45°, -45°) raster angle, the applied load is taken by all the rasters. This behavior can be explained by examining the specimens during the compressive testing as shown in Figure 14. Figure 15 represents the load vs. deformation relationship for (0°, 90°) and (45°, -45°) raster angles. According to the graph, (0°, 90°) raster specimens exhibit about 40% higher yield strength and stiffness in comparison to (45°, -45°) specimens. In the case of (0°, 90°) raster specimens, the deposited vertical rasters act as struts and resist the deformation until a load of ~43 kN, and the specimen suddenly fails internally due to buckling at ~2 mm deformation. In the case of (45°, -45°) raster specimen, the failure does not occur suddenly. The sparse specimen created with (45°, -45°) raster angle undergoes more deformation before failure occurs. The structure reaches a deformation of ~2 mm at a load of ~26 kN, which is about 40% less than the failure load of (0°, 90°) raster specimen. All of the tested samples for each set of specimens exhibit the same behavior. The

failure in the (45°, -45°) raster specimen occurs on the contour of the specimen upon continuous loading as shown in Figure 15. Thus, the (0°, 90°) raster specimen is comparatively stiffer and stronger compared to the (45°, -45°) raster specimen.

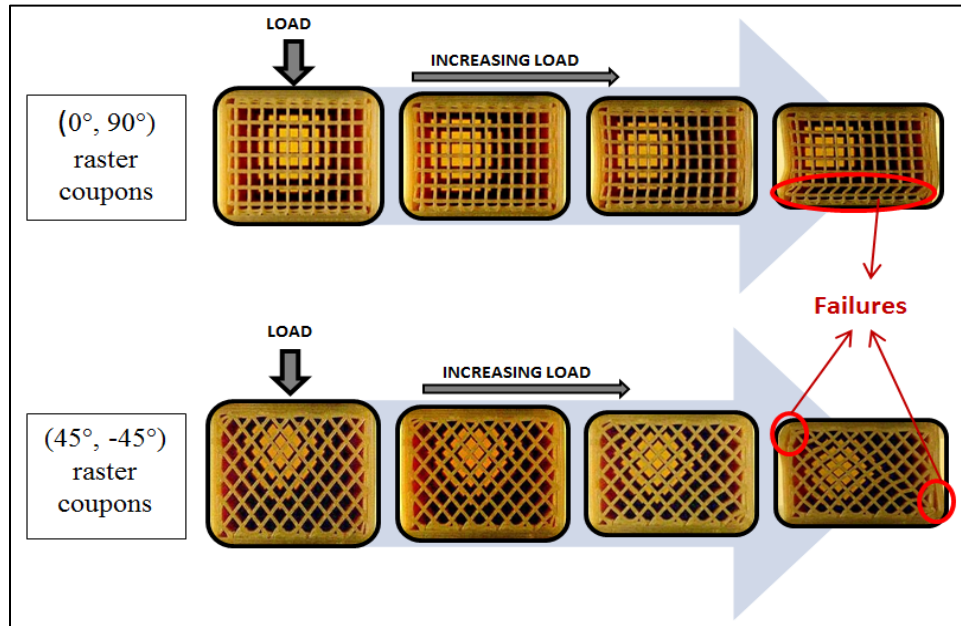


Figure 14. Gradual failure of vertical-build sparse specimens with (0°, 90°) and (45°, -45°) raster angles in compression tests

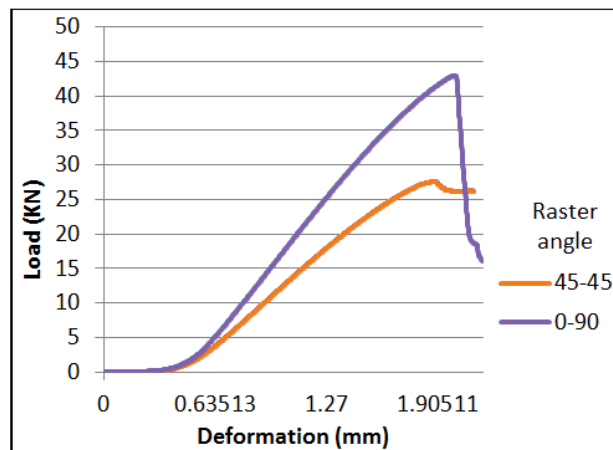


Figure 15. Load vs. deformation for vertical-build sparse specimens in compression tests

#### 4. Conclusion

The FDM process was used to fabricate solid and sparse Ultem 9085 specimens. The specimens were varied in build parameters, and compressive properties including modulus and yield strength were studied. A full-factorial experiment was utilized to determine the effects of the build parameters including build direction, raster angle, and air gap. From the statistical data,

it can be concluded that for both solid and sparse specimens, the interaction between build direction and raster angle is the most significant factor in the resulting differences in yield strength between specimens.

The compression test results indicate that the horizontal-build direction exhibits 15-40% higher compressive strength in comparison to vertical-build direction for both solid and sparse build specimens. The compressive yield strength of vertical-build solid and sparse specimens is 12-30% higher with (0°, 90°) raster angle in comparison to (45°, -45°) raster angle; however, the difference in compressive yield strength due to different raster angles was very small for horizontal-build specimens. The effect of negative air gap on the compressive yield strength was determined to be not statistically significant (p-value > 0.05) for solid specimens.

## 5. Acknowledgements

This research is sponsored by the Industrial Consortium of the Center for Aerospace Manufacturing Technologies (CAMT) at Missouri University of Science and Technology. Special thanks are due to Michael Hayes of Boeing and Timothy Schniepp and Chris Holshouser of Stratasys for their valuable contributions to the project.

## 6. References

1. Bagsik, A., Schoeppner, V., “Mechanical properties of fused deposition modeling parts manufactured with ultem 9085,” *Proceedings of the ANTEC, Plastics: Annual Technical Conference Proceedings*, ANTEC 2011.
2. Bagsik, A., Schoeppner, V., Klemp, E., “FDM part quality manufactured with ultem 9085,” *14<sup>th</sup> International Scientific Conference on Polymeric Materials*, Halle (Saale), 2010.
3. Lee, B.H., Abdullah, J., Khan, Z.A., “Optimization of rapid prototyping parameters for production of flexible ABS objects,” *Journal of Materials Processing Technology*, 169, pp. 54-61, 2005.
4. Lee, C.S., Kim, S.G., Kim, H.J., Ahn, S.H., “Measurement of anisotropic compressive strength of rapid prototyping parts,” *Journal of Materials Processing Technology*, 187, pp. 627-630, 2007.
5. Ognzan, L., Dejan, M., Miroslav, P., “Effect of layer thickness, deposition angle and infill on maximum flexural force in FDM built specimens,” *Journal for Technology of Plasticity*, Vol.39, Number 1, 2014.
6. Raut, S., Vijaykumar, S.J., Nitin, K.K., Singh, T.P., “Investigation of the effect of build orientation on mechanical properties and total cost of FDM parts,” *Procedia Materials Science*, 3<sup>rd</sup> International Conference on Materials Processing and Characterization, 6, pp. 1625-1630, 2014.

7. Panda, S.K., Padhee, S., Sood, A.K., Mahapatra, S.S., "Optimization of fused deposition modeling process parameters using bacterial foraging technique," *Intelligent Information Management*, Vol. 1, Issue 2, pp. 89-97, 2009.
8. Rayegani, F., Onwubolu, G.C., "Fused deposition modeling process parameter prediction and optimization using group method for data handling and differential evolution," *International Journal of Advanced Manufacturing Technology*, 73, pp. 509-519, 2014.
9. Anitha, R., Arunachalam, S., Radhakrishnan, P., "Critical parameters influencing the quality of prototypes in fused deposition modeling," *Journal of Materials Processing Technology*, 118, pp. 385-88, 2001.
10. Vasudevarao, B., Natarajan, D.P., Henderson, M., "Sensitivity of RP surface finish to process parameter variation," *Department of Industrial engineering*, Arizona State University, 2010.
11. Derringer, G., Suich, R., "Simultaneous optimization of several response variables," *Journal of Quality Technology*, 12(4), pp. 214-219, 1980.
12. ASTM International – D790-10, standard test methods for flexural properties of unreinforced and reinforced plastics and electrical insulating materials.
13. Buchan, E., "Stats direct: Statistical analysis – P-value", [www.statsdirect.com/p\\_values](http://www.statsdirect.com/p_values).